All-Inorganic Colloidal Perovskite Quantum Dots: A New Class of Lasing Materials with Favorable Characteristics

Yue Wang, Xiaoming Li, Jizhong Song, Lian Xiao, Haibo Zeng, and Handong Sun**

Semiconductor quantum dots (QDs) have been recognized as an advantageous optical gain material over bulk and quantum well counterparts.[1–5] By virtue of the 3D quantum confinement effect, QDs possess size-tunable emission wavelength, well-separated delta function-like density of states and large optical oscillator strength, which promises a low-threshold and temperature-insensitive optical gain.[1,6–9] Such quantum-mechanics-governed materials can be envisioned to develop single-photon sources and to be used as qubits in quantum computing.[10]

So far, the best developed and studied colloidal QDs have been fabricated from metal chalcogenide semiconductors whose crystal structure is either zinc blend or wurtzite.[7,11,12] While materials with perovskite structure have long been found to exhibit fascinating physical properties including superconductivity, ferroelectricity, and colossal magnetoresistance, etc.,[13] but they have never demonstrated impact in the fields of photonics and optoelectronics. Recently, hybrid organic–inorganic halide perovskites ($CH_3NH_3PbX_3$, X = I, Br, Cl), which are emerging as the most promising photovoltaic materials,[14,15] were discovered to be potential optical gain media.[16–18] However, these organic–inorganic halide perovskites are extremely sensitive to oxygen and moisture, which incurs constraint of a critical environment for storage, fabrication, and device operation,[17,18] commonly notorious in organic photonic materials.

Here, we present a new class of lasing materials with outstanding optical gain signatures of combined advantages of both QDs and halide perovskites: the colloidal all-inorganic cesium lead halide perovskite QDs (IPQDs) ($CsPbX_3$, X = Cl, Br, I), which were very recently reported as a high efficiency luminescent materials.[19] We observed low-threshold, wavelength-tunable, and ultrastable stimulated emission (SE) from these IPQDs at room temperature under atmospheric environment. The SE mechanism in these IPQDs was unambiguously manifested to originate from the recombination of biexcitons with high biexciton binding energy of ≈50 meV, which is definitely advantageous over the electron–hole recombination. Through detailed spectroscopy study, we attribute the physical origin of SE in these $CsPbX_3$ IPQDs with such a low threshold to the combined effects of high photoluminescence quantum yield (PL QY), ultrafast buildup of population inversion and subsequent optical amplification, the high absorption cross-section and the large Stokes shift of the SE peak. Notably, the SE wavelength of our IPQDs can be tuned across the whole visible spectral range by facilely manipulating either dot size or constituent stoichiometry, thus the optoelectronic properties can be further boosted by appropriate bandgap engineering. The attributes of flexibility and advantageous optical gain properties of colloidal $CsPbBr_3$ IPQDs were validated by demonstration of an optically pumped whispering gallery mode (WGM) microlaser. Our results indicate that these innovative IPQDs are emerging as a new research paradigm in photonics and will compete favorably with both conventional CdSe-based QDs and organic–inorganic hybrid halide perovskites as optical gain media.

The $CsPbX_3$ IPQDs adopted here were fabricated following a recipe slightly modified from the literature (see details in Experimental Section).[19] We have synthesized a series of IPQDs samples with different halide compositions and/or dot sizes. First we focus our systematic investigation on $CsPbBr_3$ IPQDs with an edge size of ≈9 nm. The UV–vis absorption and PL spectra are presented in **Figure 1**a and the transmission electron microscope (TEM) image is shown in Figure 1b. The inset in Figure 1a illustrates the cubic perovskite structure of $CsPbBr_3$ IPQDs, which is confirmed by X-ray diffraction measurements (Figure S6b, Supporting Information). The corresponding composition analysis by scanning transmission electron microscope (STEM) is shown in Figure S1 (Supporting Information). To explore the SE, the close-packed thin film of $CsPbBr_3$ IPQDs was pumped at optical wavelength of 400 nm via standard stripe pumping configuration (SPC) (inset in **Figure 2**a) with femtosecond laser pulses (100 fs, 1 kHz) (see film preparation and characterization in Supporting Information and optical characterization in Experimental Section). Figure 2a shows the evolution of PL spectra from the thin film of $CsPbBr_3$ IPQDs under varying pump intensities. It is found that the PL spectra under low pump intensities (<≈22 μJ cm^{-2}) is dominated by the relatively broad spontaneous emission located at 514.5 nm (full-width of half maximum (FWHM): ≈23 nm), while a narrower emission band located at 524.5 nm with

Y. Wang, L. Xiao, Prof. H. D. Sun
Division of Physics and Applied Physics
School of Physical and Mathematical Sciences
Nanyang Technological University
Singapore 637371, Singapore
E-mail: hdsun@ntu.edu.sg
X. M. Li, Dr. J. Z. Song, Prof. H. B. Zeng
Institute of Optoelectronics & Nanomaterials
College of Materials Science and Engineering
Nanjing University of Science and Technology
Nanjing 210094, China
E-mail: zeng.haibo@njust.edu.cn
X. M. Li
State Key Laboratory of Mechanics and Control of Mechanical Structures
College of Materials Science and Engineering
Nanjing University of Aeronautics and Astronautics
Nanjing 210085, China
Prof. H. D. Sun
Centre for Disruptive Photonic Technologies (CDPT)
Nanyang Technological University
Singapore 637371, Singapore

DOI: 10.1002/adma.201503573

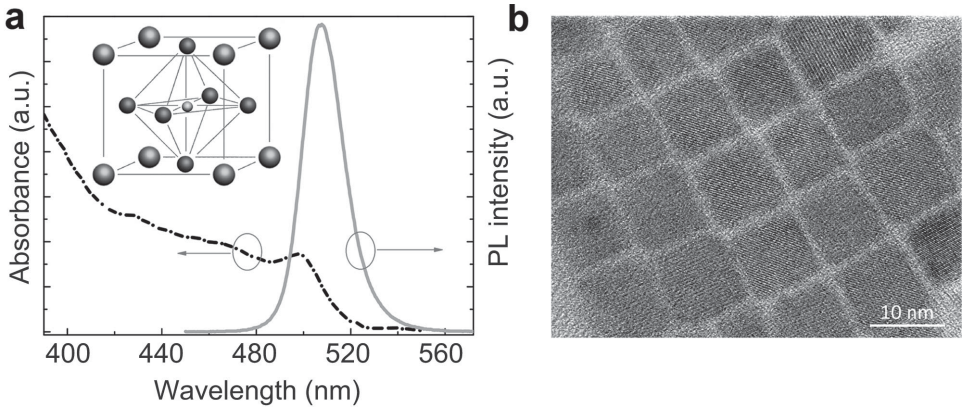

Figure 1. a) Absorption and emission spectra of $CsPbBr_3$ IPQDs in solution. Inset: Cubic perovskite structure of $CsPbBr_3$ IPQDs: Medium spheres in the centers of the cubic faces: Br; Small sphere in the center of the cubic: Pb; Large spheres in the cubic corners: Cs. b) TEM image of $CsPbBr_3$ IPQDs.

FWHM of ≈5 nm appears on the longer wavelength side when the pump intensity exceeds ≈22 μJ cm^{-2}. The plot of the integrated intensity of the sharp peak as a function of the pump intensity (Figure 1b) exhibits a super-linear increase behavior, indicating the development of SE in these $CsPbBr_3$ IPQDs.[20] The pump threshold is derived to be as low as ≈22 μJ cm^{-2}, which stands among the lowest value for colloidal QDs[7,20–22] and is nearly one order of magnitude lower than those of CdSe-based QDs emitting at similar spectral range.[7,11] The model gain coefficient of the $CsPbBr_3$ IPQDs thin film was estimated to be ≈98 cm^{-1} by the variable stripe length (VSL) method[7,23] under pump intensity of 57.0 μJ cm^{-2} (Figure S3b, Supporting Information), which is comparable to or even better than the traditional QDs[1,7,24] (≈95 cm^{-1} for red-emitting CdSe/ZnCdS QDs at 120 μJ cm^{-2} and ≈60 cm^{-1} for green-emitting counterparts at 155 μJ cm^{-2}).[7]

It is worth mentioning that the solution-processed hybrid organic–inorganic perovskites ($CH_3NH_3PbX_3$, X = I, Br, Cl) degrade rapidly when exposed to oxygen and/or moister, thus, critical working conditions are required.[17,18] For instance, the SE from $CH_3NH_3PbX_3$ films and lasing from $CH_3NH_3PbX_3$ nanowires were observed in vacuum and nitrogen atmosphere, respectively.[17,18] In contrast, our $CsPbBr_3$ IPQDs are so robust that the SE could sustain in atmospheric environment. Remarkably, even after being exposed to air for 3 weeks, the pump threshold of our sample is found to only slightly increase (Figure S3a, Supporting Information). Moreover, the SE from these $CsPbBr_3$ IPQDs shows an excellent stability upon uninterrupted laser irradiation. Figure 2c displays the SE peak intensity as a function of laser shots under pump intensity of 57.0 μJ cm^{-2} and the corresponding PL spectrum is presented in the inset. The SE intensity could retain nearly 90% of its initial value after 1.6×10^7 laser shots (≈4.5 h), which represents more than one order of magnitude longer than those of conventional colloidal QDs,[25,26] indicating the exceptional photostability of these $CsPbBr_3$ IPQDs.

Generally speaking, there are two likely SE mechanisms for colloidal QDs, namely, the single-exciton and the biexciton gain.[1,7,21] The observed largely red-shifted SE peak in our $CsPbBr_3$ IPQDs with respect to the corresponding spontaneous emission maximum might suggest the biexcitonic SE in origin.[1,7] To verify that the SE in these $CsPbBr_3$ IPQDs stems from the light amplification of biexciton emission, we investigate the PL from these $CsPbBr_3$ IPQDs using quasi-continuous wave pumping,[27,28] in which the pulse-width (5 ns) of the laser source is far longer than the Auger lifetime (≈105 ps as shown later) so as to prolong the duration of biexciton emission. Therefore, the weight of biexciton emission intensity in PL spectra is dramatically boosted.[27] Moreover, we employed the backscattering configuration (inset in **Figure 3**a) and kept at low excitation intensity to avoid the complication of reabsorption and amplification effects, and the measurements were performed at 10 K to suppress thermal broadening in order to better distinguish the biexciton emission from PL spectra. Figure 3a shows the excitation intensity-dependent PL spectra from the thin film of $CsPbBr_3$ IPQDs. Under relatively low excitation intensities (<≈3.4 mJ cm^{-2}), the PL is dominated by the typical exciton emission (Band A). With the gradual increase of excitation intensity, a new emission band (Band B) appears on the low-energy side and its weight relative to Band A increases with excitation intensity. To spectrally separate the Band A and Band B, the PL spectra are fitted by a two-peak Voigt function following the procedure similar to Moreels et al.[29] as shown in Figure 3b. Figure 3c displays the extracted spectrally integrated intensities of Band A and Band B as a function of excitation intensity from 1.2 to 17.2 mJ cm^{-2}. The linear and quadratic dependences of PL intensities of these two bands on the excitation intensity unambiguously confirm the exciton emission and biexciton emission, respectively.[29–31] The biexciton binding energy is derived to be as high as ≈50 meV based on the energy separation between exciton and biexciton peak positions (Figure 2b),[27,29,30] which is consistent with the carrier confinement effect in a QD.[11,31,32] Back to the SE spectra shown in Figure 2a, the energy separation of the spontaneous and stimulated emission bands matches well the two bands presented in Figure 3, thus it can be safely concluded that SE indeed originates from biexcitonic recombination.

In view of the thermal energy of ≈26 meV at 300 K, the binding energy of 50 meV in our IPQDs allows for biexciton state to survive well above room temperature,[11,29] which is definitely advantageous for stimulated emission over electron–hole recombination. Moreover, the large biexciton binding

Adv. Mater. **2015**,
DOI: 10.1002/adma.201503573

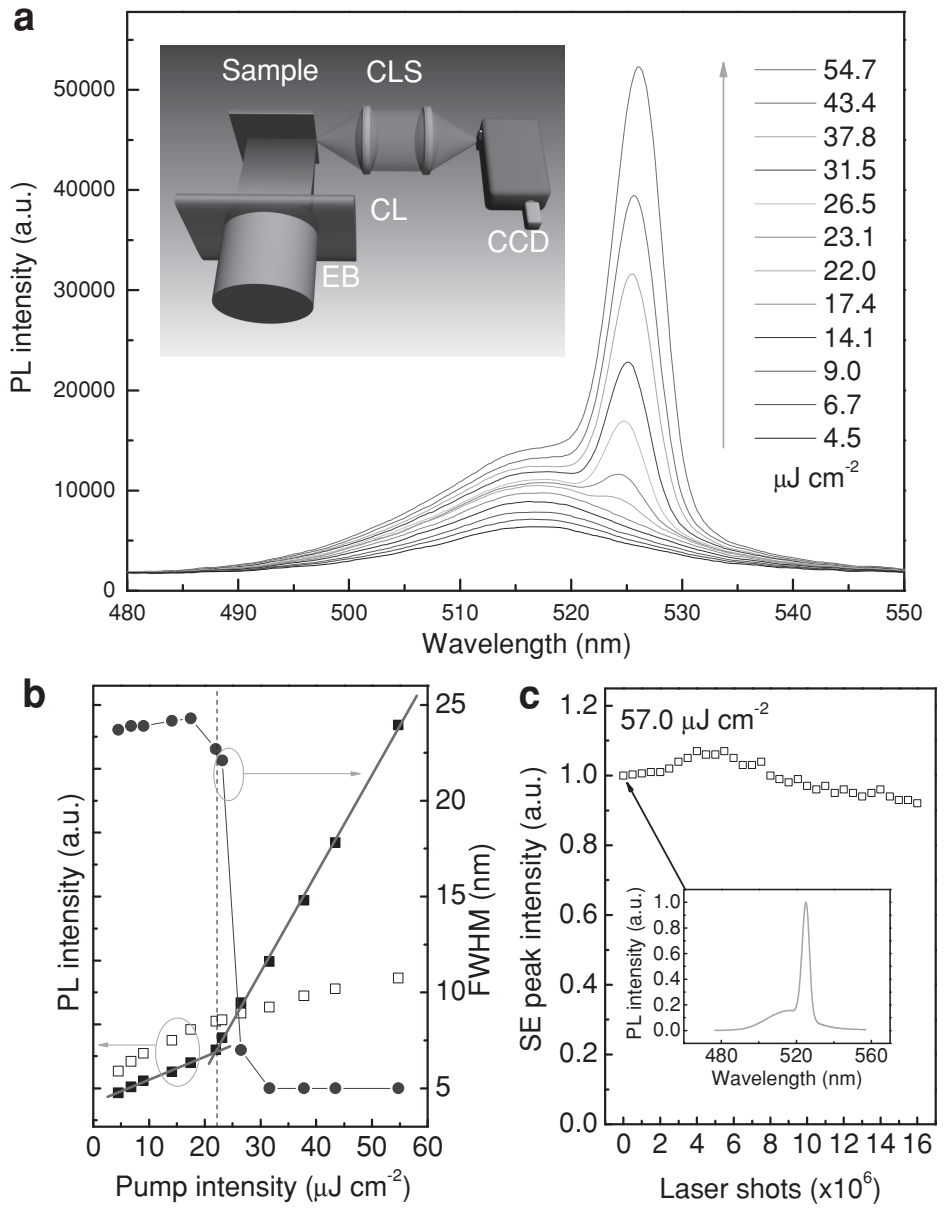

Figure 2. a) Pump intensity-dependent PL spectra from thin film of $CsPbBr_3$ IPQDs. The inset shows the stripe pumping configuration used in this measurement (excitation beam (EB), cylindrical lens (CL), collection lens set (CLS), charged coupled device (CCD)). b) The FWHM of the PL spectra (solid circles) shows abrupt narrowing and the spectrally integrated PL intensity of the sharp peak (solid squares) exhibits a threshold behavior with respect to pump intensity. The spontaneous emission peak (hollow squares) experiences saturation as the pump intensity increases. c) Plot of stimulated emission peak intensity as a function of laser shot. The inset shows the PL spectrum at beginning.

energy in these $CsPbBr_3$ IPQDs results in the large red shift of the SE peak, which would reduce the detrimental reabsorption loss and contribute to the low threshold.[29]

The superb optical gain properties of the $CsPbBr_3$ IPQDs makes them competitive as new quantum materials for lasing, especially for green and blue spectral range, where the conventional II–VI group QDs show much poorer gain performance than their red counterparts.[11] Naturally, an essential question lies in why SE could occur in these IPQDs with such a low threshold. First, the PL QY is known to strongly impact the gain performance and a high PL QY for a gain medium will contribute to a lower pumping threshold due to the reduced loss by nonradiative carrier trapping.[7,17,26] The PL QY of the $CsPbBr_3$ IPQDs is measured to be as high as 90% in solution. The PL decay of $CsPbBr_3$ IPQD solution under low pump intensity shows a nearly single exponential decay with lifetime of ≈3.6 ns (**Figure 4**a), indicating that the nonradiative carrier trapping process is insignificant in these IPQDs.[7,20] When self-assembling the IPQDs into close-packed thin film, the single-exciton lifetime slightly decreases to be ≈3.1 ns (Figure 4a), which suggests that up to ≈85% of their PL QY of $CsPbBr_3$ IPQDs are able to be preserved when transferred from solution to a thin film.[7] The high PL QY of the $CsPbBr_3$ IPQD thin film stands several times higher than those of the hybrid organic–inorganic perovskite films and crystals as well as conventional II–VI group semiconductor QD films[1,16,17,33] and certainly should be one of contributing factors towards the low-threshold SE in these IPQDs. On contrary, the low PL QY in the above-mentioned other materials, especially the bulk polycrystalline films, implies fast nonradiative recombination, thus more unfavorable heat will be generated, which plagues their optical properties and complicates thermal management for device operation.[2,6]

On the other hand, the rapid nonradiative Auger recombination occurring at high excitation intensities has been recognized to be the main channel dissipating the population inversion in QDs,[1,34] thus hindering the optical amplification. To explore Auger recombination in these $CsPbBr_3$ IPQDs, the excitation intensity-dependent time-resolved PL measurements were performed on $CsPbBr_3$ IPQDs in solution (see details in Experimental Section). As shown in Figure 4b, the PL decay of the $CsPbBr_3$ IPQDs is dictated by relatively slow single-exciton recombination under low excitation intensities (<4.5 μJ cm^{-2}), then a fast decay process emerges as the excitation intensity increases, corresponding to the Auger recombination.[1,7,35] The lifetime of the Auger process in these $CsPbBr_3$ IPQDs is derived to be ≈105 ps (Figure S4, Supporting Information). Compared to those of CdSe QDs

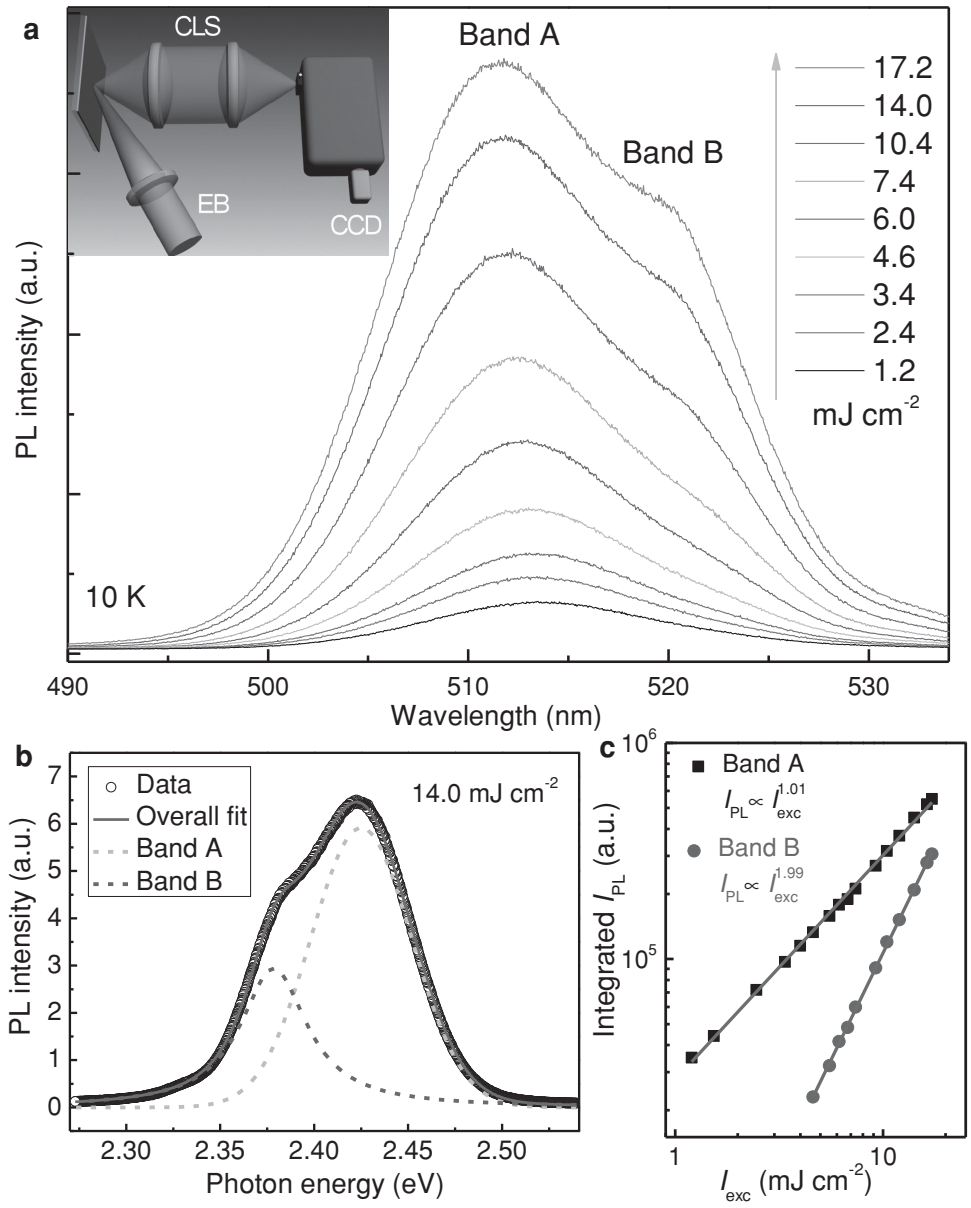

Figure 3. a) Excitation intensity-dependent PL spectra from thin film of $CsPbBr_3$ IPQDs at 10 K under nanosecond laser excitation (pulse-width: 5 ns). b) Separation of Band A and Band B from the PL spectrum. c) Spectrally integrated PL intensity of Band A and Band B as a function of excitation intensity. The lines are the linear fitting curves with slopes of 1.01 and 1.99, which confirms the exciton and biexciton emission for Band A and Band B, respectively.

emitting in similar spectral range (τ_{Auger} = ≈50 ps for CdSe QDs with diameter of ≈5 nm),[11,35] the Auger loss is somewhat mitigated in these $CsPbBr_3$ IPQDs. Deeper insights are obtained from the PL dynamic measurements on thin film of $CsPbBr_3$ IPQDs via SPC. **Figure 5**b,e, and h show the time-resolved PL spectrograms of $CsPbBr_3$ IPQD thin film under pump intensity of 0.8, 11.5, and 25.0 μJ cm^{-2}, respectively, and the spectrally integrated PL decay curves extracted from the spectrograms are presented in Figure 5c,f,i, respectively. Under low pump intensity (0.8 μJ cm^{-2}), the PL decay follows the single-exponential excitonic recombination (Figure 5c). As the pump intensity increases (11.5 μJ cm^{-2}), the rapid Auger recombination emerges in the spectrogram as the bright vertical stripe and is also seen from the PL decay curve (Figure 5f). The transient PL spectrum (0–50 ps) in Figure 5d redshifts compared to that integrated over the whole time window (0–6.0 ns), while those (Figure 5a) under low pump intensity are nearly identical, which coincides with the presence of biexciton emission under high pump intensity (11.5 μJ cm^{-2}).[7,29] While as the pump intensity (25.0 μJ cm^{-2}) just exceeds the threshold, a narrow emission band appearing on the longer wavelength side manifests as an intense ellipse spot in the spectrogram and, concomitantly, a much faster PL decay is observed (Figure 5i), indicating the development of SE. Importantly, the PL decay of the SE peak is so fast that the access of its precise time constant is limited by the resolution of the streak camera system

Adv. Mater. 2015,
DOI: 10.1002/adma.201503573

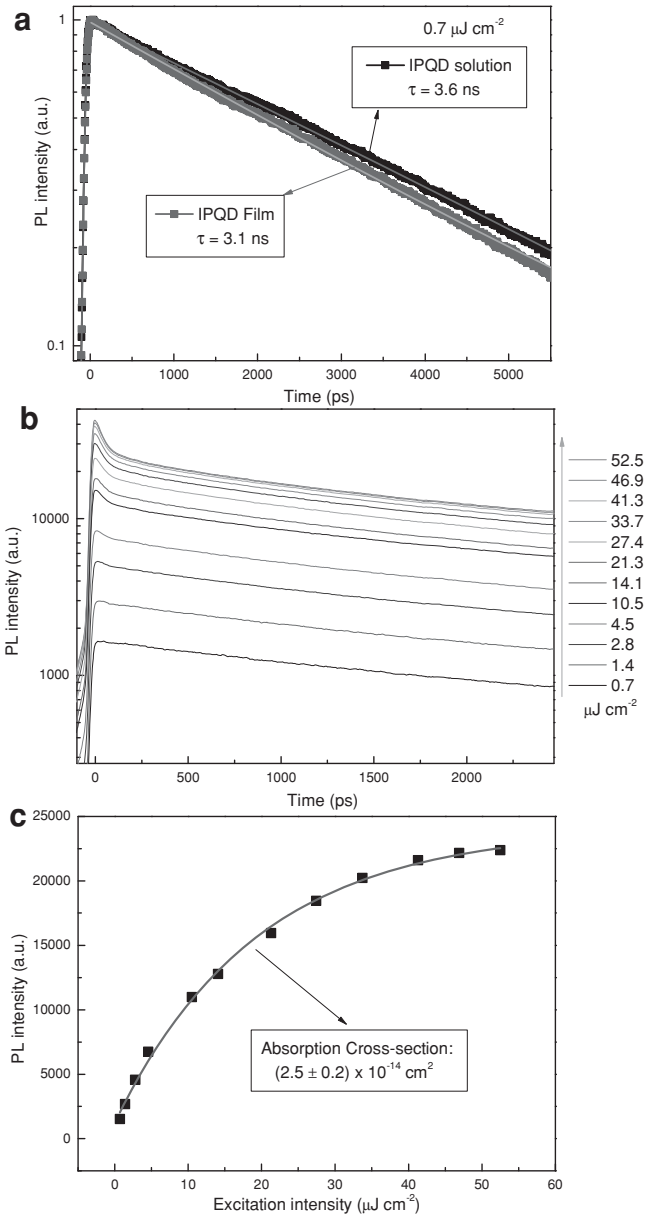

Figure 4. a) Single-exciton recombination lifetime of $CsPbBr_3$ IPQD solution and film. b) Excitation intensity-dependent PL decay traces of $CsPbBr_3$ IPQDs in solution, resolving the Auger recombination under high excitation intensities. c) PL intensity at time delay of 400 ps as a function of excitation intensity. The curve is the best-fitting line based on Poisson distribution of the number of excitons upon photoexcitation.

(≈50 ps). The transient spectra within the initial 50 ps displays a pronounced SE peak, while the PL spectra integrated over the subsequent temporal window (50 ps–6.0 ns) only show the broad spontaneous emission (Figure 5g), evidencing that the buildup of optical gain and the subsequent SE in these IPQDs takes place within a ultrashort timescale (<50 ps). In fact, as shown in the VSL measurements (Figure S3b, Supporting Information), the SE intensity saturates at long pumping stripe lengths. From the measured saturation length (≈0.07 cm) of the SE intensity, the gain depletion time is estimated to be ≈5 ps, more than one order of magnitude shorter than Auger lifetime, which is just induced by the ultrafast SE.[1,7] Therefore, even though Auger recombination may dissipate the excited carriers, the efficient SE developed in these IPQDs could easily outperform the Auger recombination.

Optical absorption is also an important factor influencing optical pumping threshold. For colloidal QDs, the intrinsic property of optical absorption ability is characterized by absorption cross-section. However, to directly extract the absorption cross-section of our IPQDs is very challenging due to the size and composition inhomogeneity and the disturbance of the indispensable surface ligands. Here we attempt to estimate the absorption cross-section (σ) of our $CsPbBr_3$ IPQDs following a well-established method for colloidal QDs.[36,37] Based on the fact that the fast Auger recombination completes within the initial hundreds of ps (τ_{Auger} = ≈105 ps), all of the excited $CsPbBr_3$ IPQDs will only contain single exciton at long-time delays, which is demonstrated by the parallel decay lines under both high and low excitation intensities without taking into account the early hundreds of ps (Figure 4b).[28,37] It is well established that the probability of the number of excitons generated in QDs follows the Poisson distribution,[11] thus, the PL intensity with long delay time is proportional to the probability of the excited QDs in the ensemble, given by $1-P_0$, where $P_0 = e^{-\sigma I/-\sigma\hbar\omega}$ is the probability of the non-excited QDs, I is the excitation intensity and $\hbar\omega$ is the photon energy at 400 nm.[37] As shown in Figure 4c, the excitation intensity-dependent PL intensity with delay time of 400 ps could be well fitted according to above analysis, from which the absorption cross-section is extracted to be ≈2.5×10^{-14} cm^2, which is much larger than those of CdSe QDs emitting at similar green range[11] but reasonable considering the big dot size and the intrinsic large absorption coefficient of the halide perovskites, thus contributing to the low threshold SE of our IPQDs. The physical reasons for both the large biexciton binding energy and the large absorption cross-section of $CsPbBr_3$ IPQDs may be related to the common intrinsic properties of perovskite materials[17,18] and quantum confinement effect,[9,32] the detail of which remains further investigation and is beyond the scope of this work.

One of the most important hallmarks of QDs is the size-tunable emission wavelength due to quantum confinement effect.[11] Correspondingly, the SE wavelength of these $CsPbX_3$ IPQDs could potentially be tailored via facile size control. **Figure 6**a displays the PL spectra from $CsPbBr_3$ IPQDs with edge length of ≈5.5 nm (see TEM image in Figure S5a, Supporting Information) under varying pump intensities. Compared to the 9 nm sized sample, 5.5 nm sized $CsPbBr_3$ IPQDs exhibit blue-shifted spontaneous (≈490 nm) and stimulated (≈502 nm) emissions, demonstrating the feasibility of size-tunable SE in these $CsPbX_3$ IPQDs. Besides, it is known that the bandgap of lead halide perovskites could be engineered by changing their constituent stoichiometries.[17,18] Here, we show that the SE from these $CsPbX_3$ IPQDs could be tuned across the whole visible spectral range by halide substitution. Figure 6b,c display the blue and red SE from $CsPb(Br/Cl)_3$ (Br:Cl = 1.15:1) and $CsPb(I/Br)_3$ (I:Br = 2.7:1) IPQDs, respectively, validating that blue, green, and red SE could be achieved from these stoichiometry controllable IPQDs. Therefore, taking advantage of both the halide perovskite nature and quantum confinement effect,[1,18] we showed two separate ways for the manipulation

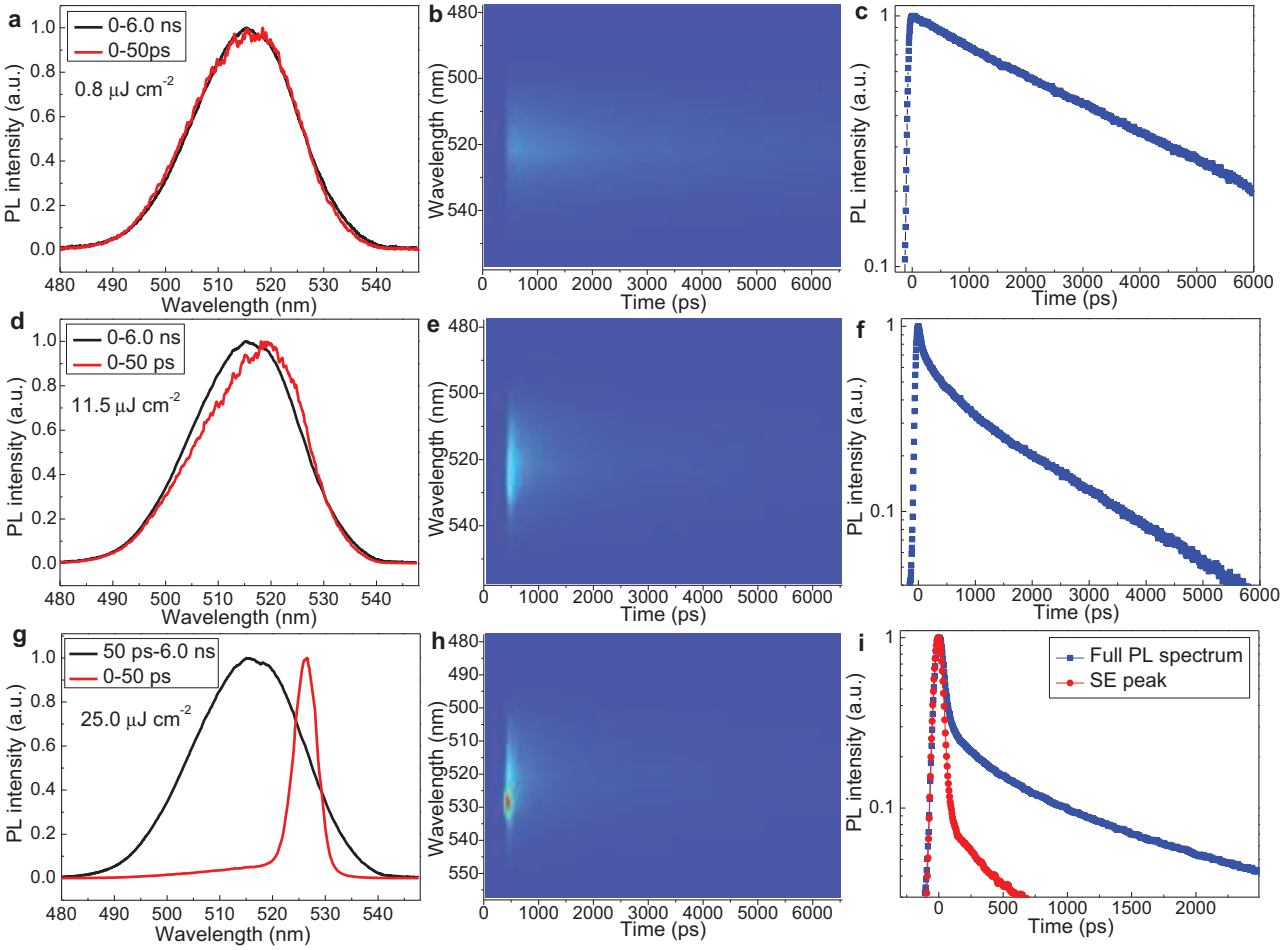

Figure 5. a–c) Time-integrated PL spectra, spectrogram, and PL decay curve under pump intensity of 0.8 μJ cm^{-2}, respectively. d–f) Time-integrated PL spectra, spectrogram, and PL decay curve under pump intensity of 11.5 μJ cm^{-2}. The red-shifted PL spectrum (0–50 ps) indicates the emergence of biexciton emission. The fast Auger recombination manifests as the bright vertical stripe in the spectrogram. g–i) Time-integrated PL spectra, spectrogram, and PL decay curves of spectrally integrated over the full spectrum and over the stimulated emission peak under pump intensity of 25.0 μJ cm^{-2}. The prominent stimulated emission for transient PL spectrum (0–50 ps) and broad spontaneous emission for that of 50 ps–6.0 ns suggest that the stimulated emission only takes place within the initial 50 ps upon photoexcitation.

of SE wavelength in these $CsPbX_3$ IPQDs, which is inspiring for both fundamental and applied research.

Given the superb optical gain performance of these $CsPbX_3$ IPQDs, lasing could be readily achieved by introducing a suitable cavity resonator.[7,38] Thanks to their colloidal nature, these IPQDs are compatible with various kinds of cavities so as to achieve lasing with different types of optical feedback.[7,38] As a demonstration, we filled the $CsPbBr_3$ IPQDs into a capillary tube and solid film around the inner wall was formed after the evaporation of solvent as has been demonstrated for traditional QDs.[24,39] Figure 6d presents the pump intensity-dependent PL spectra from a $CsPbBr_3$ IPQDs infiltrated capillary tube (see details in Experimental Section). The emergence of evenly-spaced spikes as pump intensity increases and super-linear increase of the integrated intensity with respect to pump intensity confirm the occurrence of lasing action, and the longitudinal optical modes can be well-assigned based on WGM model (Figure S7, Supporting Information), indicating the WGM lasing mechanism.[24,39]

In conclusion, we discover that the newly engineered $CsPbX_3$ IPQDs possess superior optical gain properties, representing a new class of solution processed, low-threshold, truly stable and wavelength-tunable gain materials. The solution processability of these IPQDs also makes them applicable for device fabrication from simple and cost-effective printing and spraying technologies. We envisage that these $CsPbX_3$ IPQDs will become a new research paradigm and hold new opportunity for optoelectronics in the near future.

Experimental Section

Fabrication of $CsPbX_3$ IPQDs: Typically, a mixture of 0.8 g Cs_2CO_3, 2.5 mL of oleic acid (OA), and 30 mL of octadecene (ODE) was degassed under argon flow in a 100 mL four-neck flask at 130 °C for 1 h. Then the reaction was kept at 150 °C for another 0.5 h until all the Cs_2CO_3 have reacted with OA. After cooling to room temperature naturally, the Cs-precursor was kept in a glovebox. ODE (10 mL), OA (1 mL), oleylamine (OAm, 1 mL), and 0.36 mmol of PbX_2 (X = Cl, Br and

Adv. Mater. **2015**,
DOI: 10.1002/adma.201503573

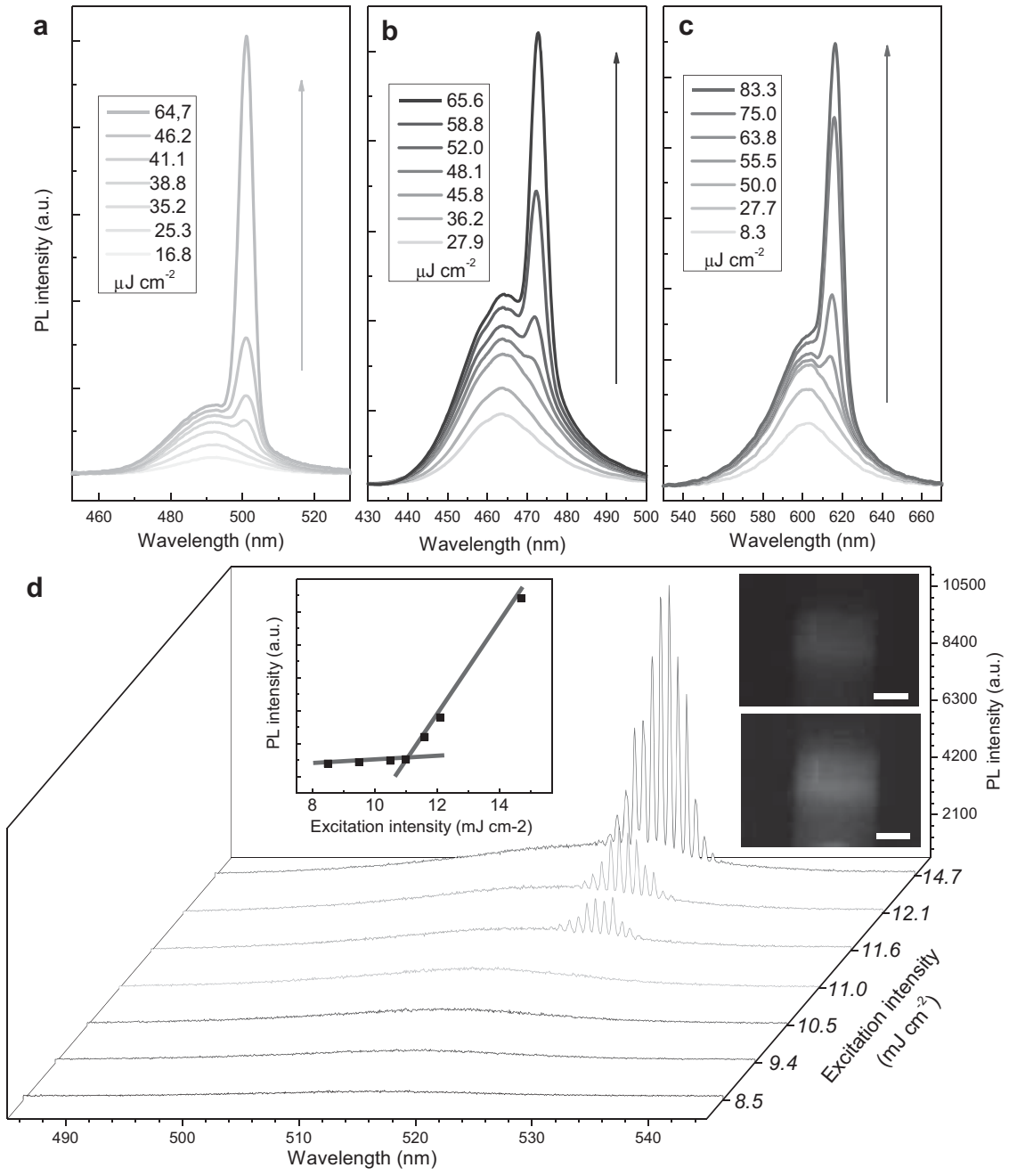

Figure 6. a) Stimulated emission from small sized-$CsPbBr_3$ IPQDs, showing blue-shifted stimulated emission wavelength. b) Blue stimulated emission from $CsPb(Br/Cl)_3$ IPQDs. c) Red stimulated emission from $CsPb(I/Br)_3$ IPQDs. d) Pump intensity-dependent PL spectra from $CsPbBr_3$ IPQDs with edge length of ≈9 nm infiltrated into a capillary tube with inner diameter of ≈50 μm. The left inset displays the spectrally integrated PL intensity over the lasing peaks with respect to pump intensity. The optical images of the IPQDs infiltrated capillary tube below (upper image) and above (lower image) the lasing threshold are presented as the right insets. Scale bar is 20 μm.

I) or their mixture were mixed and degased under argon at 130 °C for 1 h. After complete dissolution of PbX_2 salts, the temperature was raised to 160 °C and kept for another 10 min. Then, 1 mL of the Cs-precursor was swiftly injected into above hot mixture and the reaction was stopped with ice bath after 5 s. The nanocrystals were precipitated by adding excess acetone and washed with a solvent combination of toluene and acetone by centrifugation. Finally, the as prepared products were redispersed in toluene for further use. Nanocrystal size was tuned by changing the injection temperature.

Optical Measurements: For the SE measurements, a femtosecond amplified laser system was employed as the pumping source. The optical wavelength of 400 nm was generated by frequency-doubling of output pulse (Wavelength: 800 nm, Repetition rate: 1 KHz, Pulse-width: 100 fs) from regenerative amplifier using β-barium borate (BBO) crystal. The laser beam was focused vertically onto the IPQD thin film with dimension of ≈0.1 × 3 mm^2 via a cylindrical lens with focal length of 75 mm, and the emission from the edge of the film serving as the optical waveguide was vertically collected by a silicon charged coupled device

(CCD) equipped with a 320 mm monochromator. For the time-resolved PL measurements, the solution of $CsPbBr_3$ IPQDs was stored in 1 mm thick quartz cuvette and the conventional backscattering configuration was adopted for the PL collection, while those of IPQD film is the same as used in SE measurements. The emission was detected and analyzed by an Optronics streak camera system with optimized temporal resolution of ≈50 ps. In biexciton emission investigation, the IPQD film was fixed in a helium close-cycled cryostat and cooled down to 10 K. The excitation beam (400 nm, 5 ns, 20 Hz) from a wavelength-tunable nanosecond laser system was loosely focused onto the sample with diameter of ≈1 mm. The PL was dispersed by a 750 mm monochromater and recorded by a silicon-CCD. For the lasing measurements, a home-built micro-PL system was utilized. The pumping source and collection instruments are the same as those used in biexciton emission investigation.

Supporting Information

Supporting Information is available from the Wiley Online Library or from the author.

Acknowledgements

Y.W. and X. L. contributed equally to this work. All authors contributed extensively to this work. H.Z. and H.S. initialized the research. Y.W. and L.X. conducted spectroscopic experiment and analysis. X.L. and J.S. synthesized the IPQD samples. H.S. and H.Z. supervised the project. H.Z. coordinated the efforts of the research team of sample synthesis and structure characterization while H.S. leads the research efforts for optical spectroscopic characterization. Y.W., X.L., J.S., L.X, H.Z., and H.S. analyzed data, discussed and interpreted detailed results, and wrote the manuscript with input from all authors. This research is supported by the Singapore National Research Foundation through the Competitive Research Programme (CRP) under Project No. NRFCRP6-2010-02, the Singapore Ministry of Education through the Academic Research Fund under Projects MOE 2011-T3-1-005 (Tier 3) and Merlion under Project. No. 2.02.13, National Basic Research Program of China (grant number 2014CB931700).

Received: July 23, 2015
Revised: August 20, 2015
Published online:

[1] V. I. Klimov, A. A. Mikhailovsky, S. Xu, A. Malko, J. A. Hollingsworth, C. A. Leatherdale, H. J. Eisler, M. G. Bawendi, *Science* **2000**, *290*, 314.
[2] T. R. G. W. P. Risk, A. V. Nurmikko, *Compact Blue-Green Lasers*, Cambridge University Press, Cambridge, UK **2003**.
[3] A. Woolf, T. Puchtler, I. Aharonovich, T. Zhu, N. Niu, D. Wang, R. Oliver, E. L. Hu, *Proc. Natl. Acad. Sci. USA* **2014**, *111*, 14042.
[4] H. Liu, T. Wang, Q. Jiang, R. Hogg, F. Tutu, F. Pozzi, A. Seeds, *Nat. Photonics* **2011**, *5*, 416.
[5] Y. Wang, V. D. Ta, Y. Gao, T. C. He, R. Chen, E. Mutlugun, H. V. Demir, H. D. Sun, *Adv. Mater.* **2014**, *26*, 2954.
[6] R. R. Cooney, S. L. Sewall, D. M. Sagar, P. Kambhampati, *Phys. Rev. Lett.* **2009**, *102*, 127404.
[7] C. Dang, J. Lee, C. Breen, J. S. Steckel, S. Coe-Sullivan, A. Nurmikko, *Nat. Nanotechnol.* **2012**, *7*, 335.
[8] S. V. Gaponenko, *Optical Properties of Semiconductor Nanocrystals*, Cambridge University Press, Cambridge, UK **1998**.
[9] M. V. Kovalenko, L. Manna, A. Cabot, Z. Hens, D. V. Talapin, C. R. Kagan, V. I. Klimov, A. L. Rogach, P. Reiss, D. J. Milliron, P. Guyot-Sionnnest, G. Konstantatos, W. J. Parak, T. Hyeon, B. A. Korgel, C. B. Murray, W. Heiss, *ACS Nano* **2015**, *9*, 1012.
[10] A. J. Shields, *Nat. Photonics* **2007**, *1*, 215.
[11] V. I. Klimov, *Annu. Rev. Phys. Chem.* **2007**, *58*, 635.
[12] Y. Wang, S. Yang, H. Yang, H. Sun, *Adv. Opt. Mater.* **2015**, *3*, 652.
[13] A. S. Bhalla, R. Guo, R. Roy, *Mater. Res. Innovations* **2000**, *4*, 3.
[14] M. Liu, M. B. Johnston, H. J. Snaith, *Nature* **2013**, *501*, 395.
[15] M. A. Green, A. Ho-Baillie, H. J. Snaith, *Nat. Photonics* **2014**, *8*, 506.
[16] F. Deschler, M. Price, S. Pathak, L. E. Klintberg, D.-D. Jarausch, R. Higler, S. Huettner, T. Leijtens, S. D. Stranks, H. J. Snaith, M. Atatuere, R. T. Phillips, R. H. Friend, *J. Phys. Chem. Lett.* **2014**, *5*, 1421.
[17] G. Xing, N. Mathews, S. S. Lim, N. Yantara, X. Liu, D. Sabba, M. Gratzel, S. Mhaisalkar, T. C. Sum, *Nat. Mater.* **2014**, *13*, 476.
[18] H. Zhu, Y. Fu, F. Meng, X. Wu, Z. Gong, Q. Ding, M. V. Gustafsson, M. T. Trinh, S. Jin, X. Y. Zhu, *Nat. Mater.* **2015**, *14*, 636.
[19] L. Protesescu, S. Yakunin, M. I. Bodnarchuk, F. Krieg, R. Caputo, C. H. Hendon, R. X. Yang, A. Walsh, M. V. Kovalenko, *Nano Lett.* **2015**, *15*, 3692.
[20] F. Garcia-Santamaria, Y. Chen, J. Vela, R. D. Schaller, J. A. Hollingsworth, V. I. Klimov, *Nano Lett.* **2009**, *9*, 3482.
[21] V. I. Klimov, S. A. Ivanov, J. Nanda, M. Achermann, I. Bezel, J. A. McGuire, A. Piryatinski, *Nature* **2007**, *447*, 441.
[22] I. Moreels, G. Raino, R. Gomes, Z. Hens, T. Stoeferle, R. F. Mahrt, *Adv. Mater.* **2012**, *24*, OP231.
[23] C. She, I. Fedin, D. S. Dolzhnikov, A. Demortiere, R. D. Schaller, M. Pelton, D. V. Talapin, *Nano Lett.* **2014**, *14*, 2772.
[24] A. V. Malko, A. A. Mikhailovsky, M. A. Petruska, J. A. Hollingsworth, H. Htoon, M. G. Bawendi, V. I. Klimov, *Appl. Phys. Lett.* **2002**, *81*, 1303.
[25] B. Guzelturk, Y. Kelestemur, M. Olutas, S. Delikanli, H. V. Demir, *ACS Nano* **2014**, *8*, 6599.
[26] G. Xing, Y. Liao, X. Wu, S. Chakrabortty, X. Liu, E. K. L. Yeow, Y. Chan, T. C. Sum, *ACS Nano* **2012**, *6*, 10835.
[27] D. Oron, M. Kazes, U. Banin, *Phys. Rev. B* **2007**, *75*, 035330.
[28] Y. Wang, K. S. Leck, T. Van Duong, R. Chen, V. Nalla, Y. Gao, T. He, H. V. Demir, H. Sun, *Adv. Mater.* **2015**, *27*, 169.
[29] J. Q. Grim, S. Christodoulou, F. Di Stasio, R. Krahne, R. Cingolani, L. Manna, I. Moreels, *Nat. Nanotechnol.* **2014**, *9*, 891.
[30] H. D. Sun, T. Makino, Y. Segawa, M. Kawasaki, A. Ohtomo, K. Tamura, H. Koinuma, *Appl. Phys. Lett.* **2001**, *78*, 3385.
[31] B. Fisher, J. M. Caruge, Y. T. Chan, J. Halpert, M. G. Bawendi, *Chem. Phys.* **2005**, *318*, 71.
[32] F. Zhang, H. Zhong, C. Chen, X.-g. Wu, X. Hu, H. Huang, J. Han, B. Zou, Y. Dong, *ACS Nano* **2015**, *9*, 4533.
[33] Q. Liao, H. H. Zhang, X. D. Wang, J. N. Yao, H. B. Fu, *Adv. Mater.* **2015**, *7*, 133.
[34] M. Zavelani-Rossi, M. G. Lupo, R. Krahne, L. Manna, G. Lanzani, *Nanoscale* **2010**, *2*, 931.
[35] V. I. Klimov, A. A. Mikhailovsky, D. W. McBranch, C. A. Leatherdale, M. G. Bawendi, *Science* **2000**, *287*, 1011.
[36] H. Htoon, J. A. Hollingsworth, R. Dickerson, V. I. Klimov, *Phys. Rev. Lett.* **2003**, *91*, 227401.
[37] S. A. Ivanov, M. Achermann, *ACS Nano* **2010**, *4*, 5994.
[38] P. T. Snee, Y. H. Chan, D. G. Nocera, M. G. Bawendi, *Adv. Mater.* **2005**, *17*, 1131.
[39] M. Kazes, D. Y. Lewis, Y. Ebenstein, T. Mokari, U. Banin, *Adv. Mater.* **2002**, *14*, 317.